(12) INTERNATIONAL APPLICATION PUBLISHED UNDER THE PATENT COOPERATION TREATY (PCT)

(19) World Intellectual Property Organization
International Bureau

(43) International Publication Date
07 March 2024 (07.03.2024)

WIPO | PCT

(10) International Publication Number
WO 2024/049846 A1

(51) International Patent Classification:
E02F 9/14 (2006.01)

(21) International Application Number:
PCT/US2023/031437

(22) International Filing Date:
29 August 2023 (29.08.2023)

(25) Filing Language: English

(26) Publication Language: English

(30) Priority Data:
63/401,840 29 August 2022 (29.08.2022) US

(71) Applicant: **MOTION METRICS INTERNATIONAL CORP.** [US/US]; 101-2389 Health Sciences Mall, Vancouver, BC V6T 1Z3 (CA).

(72) Inventors: **TERAI, Burhanuddin, S.**; 409-2181 W 12th Avenue, Vancouver, BC V6K 4S8 (CA). **TORABI-PARIZI, Ali**; 1415 Collins Road, Coquitlam, BC V3E 0A7 (CA). **SEPEHRI, Anoush**; 42 Meadow Ridge Drive, Winnipeg, BC R3T 5N5 (CA). **KARIMIFARD, Saeed**; 1401-2628 Ash Street, Vancouver, BC V5Z 4L2 (CA). **TAFAZOLI BILANDI, Shahram**; 131 East Windsor Road, North Vancouver, BC V7N 1J9 (CA).

(74) Agent: **DZURELLA, Palmer**; ESCO GROUP LLC, 2141 NW 25th Avenue, Portland, OR 97210-2578 (US).

(81) Designated States *(unless otherwise indicated, for every kind of national protection available)*: AE, AG, AL, AM, AO, AT, AU, AZ, BA, BB, BG, BH, BN, BR, BW, BY, BZ, CA, CH, CL, CN, CO, CR, CU, CV, CZ, DE, DJ, DK, DM, DO, DZ, EC, EE, EG, ES, FI, GB, GD, GE, GH, GM, GT, HN, HR, HU, ID, IL, IN, IQ, IR, IS, IT, JM, JO, JP, KE, KG, KH, KN, KP, KR, KW, KZ, LA, LC, LK, LR, LS, LU, LY, MA, MD, MG, MK, MN, MU, MW, MX, MY, MZ, NA, NG, NI, NO, NZ, OM, PA, PE, PG, PH, PL, PT, QA, RO, RS, RU, RW, SA, SC, SD, SE, SG, SK, SL, ST, SV, SY, TH,

WO 2024/049846 A1

(54) Title: METHOD AND SYSTEM FOR MONITORING OPERATIONS OF A MINING SHOVEL

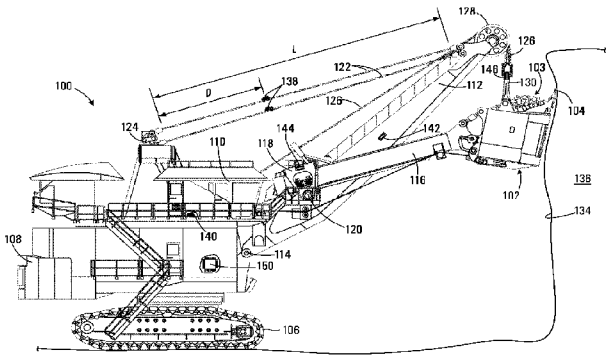

FIG. 1A

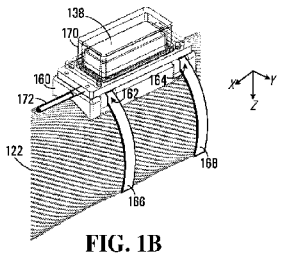

FIG. 1B

(57) Abstract: A method and system for monitoring a mining shovel having a boom supported by a plurality of suspension cables is disclosed. The method involves receiving accelerometer signals from a plurality of accelerometers, each accelerometer being mounted on one of the plurality of suspension cables. The method also involves processing the accelerometer signals to extract a fundamental frequency associated with vibration of each suspension cable, the fundamental frequency being proportional to a tension in the suspension cable. The method further involves determining changes in the fundamental frequency as a function of time, the changes being indicative of an operating state of the mining shovel.

[Continued on next page]

TJ, TM, TN, TR, TT, TZ, UA, UG, US, UZ, VC, VN, WS, ZA, ZM, ZW.

(84) **Designated States** *(unless otherwise indicated, for every kind of regional protection available)*: ARIPO (BW, CV, GH, GM, KE, LR, LS, MW, MZ, NA, RW, SC, SD, SL, ST, SZ, TZ, UG, ZM, ZW), Eurasian (AM, AZ, BY, KG, KZ, RU, TJ, TM), European (AL, AT, BE, BG, CH, CY, CZ, DE, DK, EE, ES, FI, FR, GB, GR, HR, HU, IE, IS, IT, LT, LU, LV, MC, ME, MK, MT, NL, NO, PL, PT, RO, RS, SE, SI, SK, SM, TR), OAPI (BF, BJ, CF, CG, CI, CM, GA, GN, GQ, GW, KM, ML, MR, NE, SN, TD, TG).

Published:

— *with international search report (Art. 21(3))*

METHOD AND SYSTEM FOR MONITORING OPERATIONS OF A MINING SHOVEL

Related Applications

[001] This application is claims priority benefits to U.S. Provisional Patent Application No. 63/401,840, filed August 29, 2022, entitled "METHOD AND SYSTEM FOR MONITORING OPERATIONS OF A MINING SHOVEL." This application is incorporated by reference herein in its entirety and made a part hereof.

BACKGROUND

Field of the Invention

[002] This disclosure relates generally to heavy equipment monitoring and more particularly to monitoring forces in components of a mining shovel via a determination of a frequency of vibration in suspension cables of the shovel.

Description of Related Art

[003] Large electrical mining shovels are commonly used in mining operations to load excavated ore onto haul trucks. The shovel or bucket is a critical element in the productivity of mining operations and failure or inefficient operation of the shovel can have a profound effect on ore throughput to downstream processes. Examples of mining shovels include rope shovels and dragline shovels each of which typically include a boom supported by suspension cables that support the weight of the boom and other loads. There remains a need for monitoring methods and systems that provide information on aspects such as productivity, operating health, and potential failure of mining shovels.

SUMMARY

[004] In accordance with one disclosed aspect there is provided a method for monitoring a mining shovel having a boom supported by a plurality of suspension cables. The method involves receiving accelerometer signals from a plurality of accelerometers, each accelerometer being mounted on one of the plurality of suspension cables. The method also involves processing the accelerometer signals to extract a fundamental frequency associated with vibrations in each suspension cable, the fundamental frequency being proportional to a tension in the suspension cable. The method further involves determining changes in the fundamental frequency as a function of time, the changes facilitating a determination of an operating state of the mining shovel.

[005] Receiving the accelerometer signals may involve receiving accelerometer signals from an accelerometer mounted on the suspension cable at a distance of at least one-third of the length from an end of the suspension cable.

[006] Determining changes in the fundamental frequency may involve detecting changes in fundamental frequency that are indicative of a boom jacking event associated with an excavation being performed by the rope shovel.

[007] Determining changes in the fundamental frequency may involve determining changes in fundamental frequency that are indicative of a potential failure of one of the plurality of suspension cables.

[008] The method may involve determining a tension in each of the plurality of suspension cables based on the respective fundamental frequencies relating the fundamental frequency to tension.

[009] The method may involve determining a tension in each of the plurality of suspension cables based on the respective fundamental frequencies and calibration data relating the fundamental frequency to tension.

[0010] The method may involve estimating forces on components of the mining shovel by receiving orientation signals from one or more attitude sensors associated with the components, the orientation signals defining an orientation of the components, determining a kinematic condition defining the position and orientation of the components based on the orientation signals and kinematic calibration data, and determining forces acting on the components of the mining shovel based on the kinematic condition, the orientation signals, the fundamental frequency tension in each of the plurality of suspension cables, and/or dynamic calibration data.

[0011] Estimating the forces on components of the mining shovel may involve estimating a weight of a payload in a payload container component of the mining shovel.

[0012] The method may involve performing a kinematic calibration to establish the kinematic calibration data by controlling the mining shovel to cause one of the components of the shovel to be successively located in each of a plurality of known positions and orientations with respect to the mining shovel, and processing the orientation signals based on the plurality of known positions and orientations to determine the kinematic calibration data for the mining shovel.

[0013] The method may involve performing a dynamic calibration to establish the dynamic calibration data by causing an unloaded payload container component of the mining shovel to maneuver through a trajectory while receiving the orientation signals and determining the changes in the fundamental frequency, and determining forces on the components of the mining shovel under unloaded conditions based on the changes in fundamental frequency.

[0014] The trajectory may be selected to emulate a digging operation of the mining shovel.

[0015] In accordance with another disclosed aspect there is provided a method for monitoring a mining shovel having a boom supported by a plurality of suspension cables. The method involves receiving accelerometer signals from a plurality of accelerometers, each accelerometer being mounted on one of the plurality of suspension cables at a distance of at least one-third of the length from an end of the suspension cable. The method also involves processing the accelerometer signals to extract a fundamental frequency associated with vibrations in each suspension cable, the fundamental frequency being proportional to a tension in the suspension cable. The method further involves determining changes in the fundamental frequency as a function of time, the changes facilitating a determination of an operating state of the mining shovel.

[0016] Other aspects and features will become apparent to those ordinarily skilled in the art upon review of the following description of specific disclosed embodiments in conjunction with the accompanying figures.

BRIEF DESCRIPTION OF THE DRAWINGS

[0017] In drawings which illustrate disclosed embodiments,

[0018] Fig. **1A** is a side view of a rope shovel in accordance with one disclosed embodiment;

[0019] Fig. **1B** is a perspective view of an accelerometer and a portion of a suspension cable of the rope shovel shown in Fig. **1A**;

[0020] Fig. **2** is block diagram of an embedded processor of the rope shovel shown in Fig. **1A**;

[0021] Fig. **3** is a flowchart depicting blocks of code for directing the embedded processor circuit of Fig. **2** to process the accelerometer signals generated by the accelerometer shown in Fig. **1B**;

[0022] Fig. **4A** is a graphical depiction of examples of unprocessed accelerometer signals for three different placements of accelerometer along the suspension cable of the rope shovel shown in Fig. **1A**;

[0023] Fig. **4B** is a graphical depiction of examples of a filtered, windowed, and up-sampled accelerometer signal;

[0024] Fig. **4C** is a graphical depiction of inverse autocorrelation results for a zero-crossing binary signal shown in Fig. **4B**;

[0025] Fig. **4D** is a graphical depiction of examples of f_0^2 values for a suspension cable subjected to an increasing and then reducing tension;

[0026] Fig. **5** is a schematic view of a kinematic model of the rope shovel shown in Fig. **1A**;

[0027] Fig. **6** is process flowchart example of a kinematic calibration process executed by the embedded processor circuit shown in Fig. **3**;

[0028] Fig. **7** is process flowchart example of a dynamic calibration process executed by the embedded processor circuit shown in Fig. **3**;

[0029] Fig. **8** is a schematic representation of the rope shovel of Fig. **1A** executing a simulated digging cycle; and

[0030] Fig. **9** is process flowchart example of a payload weight estimation process executed by the embedded processor circuit shown in Fig. **3**.

DETAILED DESCRIPTION

[0031] Referring to Fig. **1A**, a mining shovel is shown generally at **100**. In the embodiment shown the mining shovel **100** is a rope shovel including a dipper **102** that acts as a payload container for loading an excavated payload **103**. In other embodiments the mining shovel may be a dragline shovel that includes a payload container in the form of a bucket that is dragged to load the payload. The dipper **102** of the rope shovel **100** includes a plurality of ground engaging teeth **104** for excavating ore. The rope shovel **100** also includes a crawler track **106** and a superstructure **108** mounted for rotation on the crawler track. The superstructure **108** includes an operator's cab **110** that accommodates the shovel controls and the operator of the shovel. A boom **112** is pivotably mounted to the superstructure **108** at a boom pivot **114**. A crowd **116** is received within a saddle block **118** mounted on the boom **112** for rotation about a saddle pivot **120**. The boom **112** is supported by a plurality of suspension cables **122** connected between an upper end of the boom **112** and an A-frame **124** located on the superstructure **108**. In this embodiment, while only two suspension cables are visible due to the elevational view, there would typically be four suspension cables, each suspension cable **122** supporting a portion of the weight of the boom **112**.

[0032] The dipper **102** is pivotably mounted to a distal end of the crowd **116**. A pair of hoist cables **126** run from a winch drum (not shown) within the superstructure **108** over a pulley **128** and are coupled to either side of the dipper **102** via a bail hanger or padlocks **130**. The crowd **116** pivots within the saddle block **118** about the saddle pivot **120** when the hoist cables **126** are extended or retracted or the angle of the dipper **102** is changed. The saddle block **118** also permits the crowd **116** to be extended or retracted to force the dipper **102** into a mine face **134** of a bench **136** for excavating ore from the bench.

[0033] The suspension cables **122** support the weight of the boom **112**, the crowd **116**, the saddle block **118** and the dipper **102**. The suspension cables **122** are further subjected to load forces when excavating the mine face **134** or payload forces when carrying a payload of ore in the dipper **102**. An accelerometer **138** is coupled to each of the suspension cables **122** for generating signals representing vibrational oscillations of the respective suspension cables **122**. The suspension cables **122**, when under tension T will tend to vibrate at a frequency that is proportional to the square root of the tension and inversely proportional to the length L of the cable extending between the A-frame **124** and the end of the boom **112**. The tension in each suspension cable **122** is thus proportional to its fundamental harmonic frequency, which

in turn is a function of the length *L* of the cable. The tension in each of the suspension cables **122** may be estimated by processing the signals generated by the respective accelerometers **138** to extract a value for the fundamental frequency of vibration associated with the cable. In one embodiment, the tension T in each suspension cable **122** may be written in the form:

$$T = \alpha f_0^2 + \gamma; \qquad \text{Equation 1}$$

where α is a function of the linear density and length *L* of the suspension cable **122**, γ reflects the sag-extensibility and bending stiffness properties of the rope, and f_0 is the fundamental frequency of vibration of the cable determined from the accelerometer signal. The tension *T* is thus proportional to f_o^2. If it is desired to determine the actual tension *T* in the suspension cables **122**, the constants α and γ may be empirically determined in a calibration process or calculated from characteristics of the cable **122** such as the mass, length, cross-sectional area, Young's (elastic) modulus, and moment of inertia.

[0034] Referring to Fig. **1B**, the accelerometer **138** and a portion of the suspension cable **122** are shown in enlarged detail. In one embodiment the accelerometer **138** may be a triaxial accelerometer sensor element that measures vibration in three orthogonal axes (X,Y,Z). One example of a suitable accelerometer is the Kistler 8763 integrated electronics piezoelectric triaxial accelerometer available from Kistler Instrument Corp. of Amherst NY, USA. The accelerometer sensor element **138** is mounted on a base **160**, which in this embodiment is configured for mounting to various cables of diameters ranging from about 60 mm to 115 mm. The base **160** includes slots **162** and **164** for receiving straps **166** and **168** that secure the base to the suspension cable **122**. A cover **170** encloses the accelerometer **138** to prevent ingress of dust and debris into the sensor enclosure. In one embodiment, the accelerometer **138** is connected via a cable **172** that provides power to the accelerometer and carries generated accelerometer signals back to a control room of the rope shovel **100**. In other embodiments the respective accelerometers **138** may be powered by a battery and signals may be transmitted wirelessly to the control room of the rope shovel **100**.

[0035] Referring back to Fig. **1A**, in the embodiment shown the rope shovel **100** includes an embedded processor circuit **150** for receiving and processing the accelerometer signals from the accelerometers **138**. A block diagram of the embedded processor circuit **150** is shown in Fig. **2**. Referring to Fig. **2**, the embedded processor circuit **150** includes a microprocessor **200**, a memory **202**, and an input output port (I/O) **204**, all of which are in communication with the microprocessor **200**. In other embodiments (not shown), the embedded processor circuit **150** may be partly or fully implemented using a hardware logic circuit including discrete logic circuits and/or an application specific integrated circuit (ASIC), for example.

[0036] The embedded processor circuit **150** also includes a mass storage unit **208** such as a hard drive or solid state drive in communication with the microprocessor **200**. Program codes for directing the microprocessor **200** to carry out functions related to monitoring conditions associated with the mining shovel **102** may be stored in the memory **202** or the mass storage unit **208**.

[0037] The I/O **204** includes an interface **220** for receiving the accelerometer signals from the respective accelerometers **138**. In this embodiment, each of the accelerometers **138** are connected via a signal conditioner **230** to the respective inputs **222** – **228**. The signal conditioner **230** acts as a power supply for the accelerometers **138** and also receives, conditions and amplifies low signal level analog accelerometer signals produced by the accelerometers to generate a ±**10**V analog output signal. The interface **220** of the I/O **204** includes an analog to digital converter that is configured to covert the conditioned analog accelerometer signals into digital representations thereof for processing by the microprocessor **200**. In embodiments where the accelerometers **138** are configured for wireless transmissions, the I/O **204** would include a wireless radio in place of or in addition to the interface **220** for receiving wirelessly transmitted accelerometer signals.

[0038] In this embodiment, the I/O **204** also includes an interface **240** having an output **242** for producing display signals for driving a display **250**. The display **250** may be located in the operator's cab **110** of the rope shovel **100**. In one embodiment the display **250** may be implemented as a touchscreen display and the interface **240** may also include a USB port **244** in communication with a touchscreen interface of the display for receiving inputs from an operator. The I/O **204** may alternatively have additional USB ports (not shown) for connecting a keyboard and/or other peripheral interface devices.

[0039] Referring to Figure **3**, a flowchart depicting blocks of code for directing the microprocessor **200** to process the accelerometer signals is shown generally at **300**. The blocks generally represent codes that may be read from the mass storage unit **208** or memory **202** for directing the microprocessor **200** to perform various signal processing functions. The actual code to implement each block may be written in any suitable program language, such as C, C++, C#, Java, and/or assembly code, for example.

[0040] Block **302** directs the microprocessor **200** to receive the analog accelerometer signal from one of the inputs **222** – **228** of the interface **220**. The signals at the inputs **222** – **228** have been conditioned by the signal conditioner **230** but are otherwise unprocessed raw signals generated by the respective accelerometers **138**. For embodiments where the accelerometer **138** is a tri-axis accelerometer, separate signals are generated for each of the X-axis, Y-axis and Z-axis directions (shown in Fig. **1B**). For the mounting condition shown in Fig. **1B**, the Z-axis is directed generally downwardly with respect to the suspension cable **122**. This Z-axis direction is much more closely aligned with the direction of gravitational forces

than either the X-Axis or Y-axis directions. It is thus expected that gravitational forces on the suspension cables **122** would provide increased excitation of the harmonic modes of vibration of the respective cables and result in stronger signals. The amplitude of the Z-axis signal will generally be substantially larger than the X-Axis and Y-axis signals. In the embodiments described herein, the Z-axis signals are received as the respective analog accelerometer signals at the inputs **222 – 228**.

[0041] Referring back to Fig. **1A**, in this embodiment each of the accelerometers **138** is located a distance *D* from an end of the suspension cable **122** connected to the A-frame **124**. Referring to Fig. **4A**, examples of unprocessed Z-axis accelerometer signals for three different placements of the accelerometer **138** along the cable **122** are shown generally at **402**, **404**, and **406**. The signal **402** is produced when the accelerometer **138** is placed at $D = \boldsymbol{0.25}L$, the signal **404** is for the accelerometer placed at $D = 0.33L$, and the signal **406** is for the accelerometer placed at $D = \boldsymbol{0.4}L$. When the accelerometer **138** is placed at a location where $D < 0.33L$, the accelerometer signal is substantially attenuated as in the case of the signal **402**. The same effect applies if the accelerometer **138** is placed at the other end of the suspension cable **122** proximate the pulley **128**. Placement of the accelerometer **138** at $0.33L \leq D < 0.5L$ was found to effectively negate this attenuation effect as in the case of the signals **404** and **406**. In the embodiments described below the signals are generated for the accelerometer placement at $D = 0.33L$.

[0042] Referring back to Fig. **3**, block **302** further directs the microprocessor **200** to cause the interface **220** to perform analog to digital conversion on the signal **404**. In one embodiment the interface **220** samples the analog signal at a sampling rate of 5 kHz to generate a sampled digital signal version of the analog accelerometer signal, but other variations are possible.

[0043] The process **300** then continues at block **304**, which directs the microprocessor **200** to filter the digital accelerometer signal to remove higher harmonics. Typical suspension cables **122** have strong first and second harmonics with third and higher harmonics being substantially attenuated. For an example of a typical suspension cable **122** having a length of about 20 meters, the fundamental frequency under tension may be in the region of about 4 Hz and the filter may be configured to have a cutoff frequency at about 12 Hz, which effectively removes the third and higher harmonics. In other embodiments the material suspension cable **122** may result in higher order harmonics that have significant amplitude, in which case the filter block **304** may be configured differently to include these harmonics. In some embodiments the filtering performed at block **304** may be implemented as a band pass filter in which frequencies lower than an expected fundamental frequency are also removed by filtering. In one example, the low cut-off may be at a frequency of about 0.5 Hz to remove DC offset from the signal, but other frequencies may be used.

[0044] Block **306** then directs the microprocessor **200** to multiply the digital samples in the signal **404** by a finite-length window to generate a waveform that may be digitally processed to extract the cable tension *T*. In this embodiment the window has a duration of about **2** seconds, which for a suspension cable **122** that has a fundamental vibration frequency of at least 4 Hz will capture at least two periods of the fundamental harmonic. The window duration is selected to provide a sufficiently long sample of the accelerometer signal to facilitate extraction of the fundamental frequency of the cable vibration. The window length is a parameter that may also be adjusted to improve computational speed.

[0045] Block **308** then directs the microprocessor **200** to up-sample the filtered signal to provide a finer time spacing between adjacent discrete sample values. For the above example of a 5 kHz sampled signal **404**, the adjacent sample values are separated by 200 microseconds, but other frequencies may be used. By up-sampling the signal **410** to 100 kHz, additional sample values are generated, thus reducing the sample spacing to 10 microseconds. The up-sampling process may involve interpolating between adjacent sample values of the signal to generate the additional samples spaced at 10 microsecond intervals.

[0046] Examples of a filtered, windowed, and up-sampled signal from one of the accelerometers **138** is shown graphically in Fig. **4B** at **410**. Referring to Fig. **4B**, the accelerometer signal in this case includes two superimposed sinusoidal vibration harmonics with third and higher harmonics having been substantially removed by the filtering block **304**. While the signal **410** is shown as a continuous line, it should be understood that this is a digital signal comprising a plurality of discrete time-sampled values spaced apart by about 10 microseconds. In this case, a windowing function has also been applied and the digital signal extends in time between 0 and 2 seconds.

[0047] Block **310** then directs the microprocessor **200** to extract all of the zero-crossings in the signal **410**. In this embodiment, the zero-crossing information is generated in the form of a binary signal **412**. The binary signal **412** transitions from binary **0** to binary **1** at each zero-crossing from negative to positive. The binary signal **412** also transitions from binary **1** and binary **0** at each zero-crossing from positive to negative. These transitions are indicated by the broken lines in Fig. **4B**, shown for the first few cycles of the signal **410**. The up-sampled version **410** of the signal **400** facilitates a more accurate zero-crossing determination than would be the case if the 5 kHz sampled signal **404** were to be processed at block **310**.

[0048] Block **312** then directs the microprocessor **200** to perform a bitwise autocorrelation between the zero-crossing binary signal **412** and a delayed copy of the same signal. A delay that produces a highest autocorrelation result yields an optimal estimate for the periodicity of the signal **410**. The estimated periodicity may then be used to determine the frequency of the

fundamental vibration of the suspension cable **122** and thus the tension *T* (using equation **1** above).

[0049] In one embodiment, the autocorrelation may be efficiently computed by performing a series of bitwise exclusive OR (XOR) operations between the original zero-crossing binary signal **412** and a copy of the signal **412** delayed to each subsequent rising edge of the original signal. The delayed copies of the zero-crossing binary signal **412** may be zero padded to prevent detection of subharmonic frequencies. The closest match between the delayed signal **412** and original signal produces the smallest XOR result. The original zero-crossing binary signal **412** and the delayed copy of the signal may be encoded as a **32-bit** or **64-bit** integers, which facilitates performing a computationally efficient single XOR operation for each autocorrelation on the microprocessor **200**. In contrast, performing an autocorrelation on the accelerometer signal **410** would be significantly more computationally expensive than the simplified binary signal **412**. Performing the autocorrelation on the zero-crossing binary signal **412** also has the effect of removing any variability due to changes in amplitude of the signal **410**.

[0050] Block **314** then directs the microprocessor **200** to select the minimum autocorrelation value as an estimate of the fundamental frequency of vibration f_0 of the suspension cable **122**. In one embodiment the bitwise autocorrelation is performed as follows:

$$XOR_{SUM} = \sum XOR(original\ bitstream, delayed\ bitstream), \text{ and}$$

$$Periodicity = \frac{1}{\max\left(XOR_{SUM}, 1\right)}$$

where the periodicity thus assumes a value between 0 and 1 and where 1 indicates a perfect match. Referring to Fig. **4C**, periodicity results for the zero-crossing binary signal **412** are graphically depicted as a function of the delay time at **420**. The maximum periodicity value occurs at a point **422** having an associated time of 0.2905 seconds. This corresponds to the minimum autocorrelation value indicative of the closest match between the delayed signal **412** and original signal that provides the periodicity of the signal. Referring back to Fig. **4B**, the first rising edge **414** of the zero-crossing binary signal **412** occurs at a time of **0.0698** seconds. The fundamental frequency may thus be calculated from the period provided by the autocorrelation as follows:

$$f_o = \frac{1}{Period} = \frac{1}{0.2905 - 0.0698} = 4.52960 \text{ Hz.}$$

From the value of f_0, the frequency of the fundamental frequency of vibration of the suspension cable **122** above may then be used along with determined values for the α and γ constants in Equation **1** to yield the tension of the suspension cable **122**. The process blocks **302 – 312** thus yield a single value of f_0 for the example of the 2-second windowed time interval above.

[0051] Blocks **302** to **312** may then be continuously repeated for further 2-second windowed samples of the accelerometer signal to yield an ongoing plurality of f_0 estimates. In one embodiment the process **300** may be repeated at a rate of about 3 Hz to 10 Hz.

[0052] Referring to Fig. **4D**, examples of a f_0^2 values for a cable subjected to an increasing and then reducing tension are shown generally at **430**. A series of f_0^2 values determined in accordance with the process **300** are shown at **432**. The f_0^2 values **430** include some frequency impulse noise that may be imparted by higher frequency external stimuli. The impulse noise may be substantially eliminated by performing a median filtering of the f_0^2 values to yield the filtered values shown at **434** in Fig. **4D**. Median filtering is effective in removing impulse noise. The filtered values **434** in Fig. **4D** show a relatively smooth progression in f_0^2 and may thus be taken as being proportional to the tension T applied to the cable.

[0053] In one embodiment, filtered f_0^2 values may be monitored to reveal issues associated with the structural integrity of the suspension cables **122** and other structural elements such as the boom **112**. Rope shovels are subject to a structural fatigue process known as boom jacking, which may result in fatigue of structural elements leading to cracking or other potential component failures, e.g. the cables 122. Referring back to Fig. **1A**, when excavating the mine face **134** of the mining bench **136**, the crowd **116** is initially extended to force the ground engaging teeth **104** of the dipper **102** into the mine face and the hoist cable **126** is retracted to raise the bail hanger **130** into the orientation shown. Excavating forces on the crowd **116** or bail hanger **130** may cause the boom **112** to initially stall in the mine face **134** and then rapidly release. This rapid release may cause the boom **112** to snap backwards subjecting the boom and cables **122** to large vibrations that may be detrimental to the shovel **100**.

[0054] In one embodiment, a potential boom jacking event may be detected by monitoring the f_0^2 values for stall events (i.e. high f_0^2 values) and/or release events (i.e. rapidly reducing f_0^2 values). This pattern may be detected in the f_0^2 values and a warning issued to the operator. Alternatively, some rope shovels may be configured with an ability to automatically compensate crowding and bail hanger forces. This automatic compensation may be activated based on a detection of a potential boom jacking event from the f_0^2 values to prevent a possible boom jacking event from occurring.

[0055] The f_0^2 values also provide information that may be monitored over time to detect issues in the structural integrity of the suspension cables **122**. By monitoring f_0^2 values over successive dig cycles for each of the plurality of suspension cables **122**, a change in cable tension occurring in one or more of the cables may be indicative of a potential structural issue. For example, if the tension indicated by the f_0^2 values for one cable decreases over time while the tension on other cables increases over time. This condition may be caused by a structural issue on the cable having the reducing tension over time, such as wearing or beginning of a yield failure, or from individual strands of the suspension cables 122 fracturing.

[0056] In the above embodiments where changes in tension are inferred from changes in f_0^2 values, the constants α and γ need not be determined since the f_0^2 values are directly proportional to cable tension. As disclosed above the constants could alternatively be estimated or calculated from characteristics of the cable **122** if it is desired to determine an actual approximate tension in each cable **122**. The actual tension may be useful in determining forces on the components of the rope shovel **100** or in other applications such as payload monitoring. However, in practice slight differences in characteristics between the plurality of cables **122**, such as the exact length of each cable, may reduce the accuracy of determined tension T. In one embodiment the constants α and γ may be determined in a calibration process that accounts for variations between the plurality of cables.

[0057] Referring back to Fig. **1A**, in the embodiment shown the rope shovel **100** further includes a plurality of attitude sensors disposed on components of the shovel to measure the orientation of these elements with respect to the Earth. The plurality of attitude sensors include an attitude sensor **140** mounted in the operator's cab **110** to provide the roll, pitch, and yaw (swing) of the operator's cab **110**. The plurality of attitude sensors also include a boom attitude sensor **142** on the boom, a saddle attitude sensor **144** on the saddle block **118**, and a bail hanger attitude sensor **146** on the bail hanger **130**, which provide the orientation signals representing the orientation of these components. The attitude sensors **140 – 146** may be implemented using Inertial Measurement Unit (IMU) sensors that include 3-axis accelerometers, gyroscopes, and magnetometers, to provide real-time 3D orientation signals that identify the attitude of the respective components to which the sensor is attached. An example of a suitable IMU sensor is the VN-100 IMU/AHRS sensor available from Vectornav of Dallas, TX, USA. The VN-100 IMU/AHRS sensor generates a signal in either ASCII or binary format that identifies the attitude of the sensor.

[0058] Referring back to Fig. **2**, in the embodiment of the embedded processor circuit **150** shown, the I/O **204** includes data inputs **252 – 258** for receiving the orientation signals from the respective attitude sensors **140 – 146**. The respective orientation signals received at the data inputs **252 – 258** facilitate computation by the microprocessor **200** of the rectilinear and angular position, velocity, and acceleration of the above components of the rope shovel **100** in real time based on a kinematic model including the various linkages of the rope shovel **100**.

[0059] Referring to Fig. **5**, a kinematic model representation of the rope shovel **100** is shown generally at **500** with the rope shovel **100** shown for reference in the background. A ground coordinate frame **502** (x_0, y_0, z_0, where y_0 is aligned extending out of the plane of the page) has an origin at G and acts as a global frame of reference for the kinematic model. A shovel coordinate frame **504** (x_1, y_1, z_1) has an origin at O and represents the orientation of the superstructure **108** and operator's cab **110** with respect to the ground coordinate frame **502**. The shovel coordinate frame **504** is displaced from the ground coordinate frame **502** by a

distance indicated by the line *GO*. The orientation signal generated by the attitude sensor **140** in the operator's cab **110** provides the real-time orientation of the shovel coordinate frame **504** with respect to the ground coordinate frame **502**. In Fig. **5** the shovel coordinate frame **504** is shown in alignment with the ground coordinate frame **502**, but in practice the shovel coordinate frame may be pitched at an angle q_P or rolled at an angle q_R with respect to the ground coordinate frame **502** and may also be rotated about the z_1 axis depending on a swing angle q_w about the z_1-axis between the superstructure **108** and the crawler track **106**.

[0060] The boom **112** is represented in the kinematic model **500** by a line *BV* extending along the boom from the boom pivot **114** located at the coordinate frame (x_2, y_2, z_2) to the center *V* of the pulley **128**. The boom **112** is disposed at an angle q_B about the z_2-axis which extends out of the plane of the page. The boom angle q_B may be calculated by the microprocessor **200** from the orientation signal generated by the boom attitude sensor **142**. The saddle pivot **120** is located at an origin *L* of a saddle coordinate system (x_3, y_3, z_3) disposed along the line *BV*. The saddle is oriented at an angle about the z_3-axis which also provides the angle q_S of the crowd **116**. A point *S* on the saddle is displaced by the line *LS* from the saddle pivot **120** (*L*) and the crowd **116** extends outwardly through the point *S* and terminates at a point *C* at the end of the crowd. The extension of the crowd **116** caused by movement of the crowd through the point *S* on the saddle block **118** is represented by a variable r_C (i.e. the distance between *S* and *C*). The crowd angle q_S may be calculated by the microprocessor **200** based on the orientation signal generated by the saddle attitude sensor **144**. In other embodiments the saddle attitude sensor **144** may be placed on the crowd **116** since the saddle **118** and crowd will be disposed at the same angle.

[0061] The dipper **102** is pivotably connected to the crowd **116** at the point *C*. An angle Θ_{CH} of the dipper **102** is defined between the line *SC* and a line *CH* extending between the origin *C* and the connection between the bail hanger **130** and the dipper. The tips of the plurality of ground engaging teeth **104** are located at a point *E* with respect to the bail hanger connection *H*.

[0062] From the center of the pulley at *V*, a line *VU* defines the offset between the pulley center and the hoist cable **126**. The hoist cable **126** extends perpendicular to the line *VU* along a line *UH* extending between the bail hanger **130**. The length of the line *UH* is represented by the variable r_H corresponding to the length of the hoist cables **126** when played out from the winch drum. The line *UH* is at an angle β with respect to the vertical. The angle β is provided by the orientation signal generated by the bail hanger attitude sensor **148**.

[0063] The kinematic model of Fig. **5** may be used in conjunction with the orientation signals received from the attitude sensors **140 – 146** to determine the location of the various shovel components. The angles q_B, q_S and β are calculable from information contained in the signals generated by the attitude sensors **142 – 148**. The variable crowd extension r_C and the hoist

cable extension r_H may be determined from the kinematic model following a calibration procedure detailed below. The distances *OB*, *BL*, *LS* and *VU* may be measured or determined from a specification of the rope shovel **100**. The distance *CH* may be configured according to a desired rake angle and tooth angle at the operating site. The remaining parameters *CH* and Θ_{CH} may be determined in a kinematic calibration process. During installation, the sensors **142 – 146** may be offset or oriented at an angle that differs from the actual q_B, q_S, or β angles of the boom **112**, saddle block **118** and crowd **116**, and bail hanger **130** and the calibration process may also take these offsets into account.

[0064] Referring to Fig. **6**, a process flowchart example of a kinematic calibration process executed by the microprocessor **200** that may be implemented for the rope shovel **100** is shown generally at **600**. The process begins at **602** when the operator of the rope shovel **100** positions the ground engaging teeth **104** of the dipper **102** in a known location within the ground coordinate frame **502**. As an example, the dipper **102** may be lowered and angled as shown in Fig. **5** in broken outline at **506** until the teeth **104** engage the ground at a point P_0 within the $x_0 – z_0$ plane of the ground coordinate frame **502**.

[0065] Block **604** then directs the microprocessor **200** to receive the orientation signals from the attitude sensors **140 – 146** which provides values for the angles q_B, q_S and β. Block **606** directs the microprocessor **200** to determine whether data has been generated for all points P_0 to P_4 to facilitate calibration calculations. The distances *OB*, *BL*, *LS* and *VU* may be measured or determined from a specification of the rope shovel **100**. In this embodiment the distance *CH* and the angle Θ_{CH}, which may vary from the specification based on user configuration, may be calculated along with any sensor offsets and misalignments. In the embodiment shown, a single point P_0 does not provide sufficient data to uniquely calculate the unknown parameters (q_B, q_S, β, *CH*, Θ_{CH}, r_c and r_H). In this embodiment block **604** is repeated for five different points P_0 to P_4.

[0066] If at block **606** there remain further points to be processed, the microprocessor **200** is directed to block **608** where the operator controls the shovel to position the teeth **104** of the dipper **102** at the next point on the ground. Block **604** is then repeated for each subsequent point P_2 to P_4. At block **606**, when data for the point P_4 has been generated, the microprocessor **200** is directed to block **610**.

[0067] Block **610** then directs the microprocessor **200** to calculate the kinematic parameters including parameters *CH* and Θ_{CH}, the crowd extension r_c, and the hoist extension r_H based on the angles q_B, q_S and β and based on the ground engaging teeth **104** being located within the ground coordinate frame **502** at the respective points P_0 to P_4. Block **610** also directs the microprocessor **200** to store the determined parameters for the kinematic model **500** in the memory **202** for later use. These kinematic parameters permit the location of the components

of the rope shovel **100** shown in Fig. **5** to be computed for any combination of the angles q_B, q_S and β received in real time from the attitude sensors **140 – 148**.

[0068] Generally for a mining shovel **100**, the shovel is propelled via the crawler track **106** to position it with respect to the face **134** of the mining bench **136**. The crawler track **106** is generally not further actuated during a digging operation on the mine face **134**. The pitch and roll of the superstructure **108** and operator's cab **110** may vary during digging depending on the level and orientation of the ground engaged by the crawler track **106**, interactions of the dipper **102** with the bench face, and any changes in the center-of-mass of the dipper and payload due to movement of the shovel components. The rotation of the boom **112**, while not directly actuated, is also considered during digging operations to characterize boom jacking. Digging movements of the mining shovel **100** include actuated movements in three axes of the hoist cables **126**, the crowd **116**, and lateral swinging about the z_1=axis (i.e. the q_W angle). A state vector $\boldsymbol{q}$ may be used to describe the generalized coordinates corresponding to the degrees of freedom of the rope shovel **100**:

$$\boldsymbol{q} = \begin{Bmatrix} q_P \\ q_R \\ q_W \\ q_B \\ q_S \\ \beta \end{Bmatrix}$$

with parameters as follows:

q_P for cab pitch, rotation about y_1;

q_R for cab roll, rotation about x_1;

q_W for swing orientation, rotation about z_1;

q_B for boom orientation, rotation about z_2;

q_S for crowd orientation, rotation about z_3; and

β for bail angle, with respect to the vertical.

[0069] The displacement of the crowd **116** r_C and extension of the hoist cables **126** r_H, may be determined using the process **600** to resolve the kinematic model of Fig. **5**, and are therefore not independent. The equations of motion characterizing the shovel dynamics may be expressed as follows:

$$\mathbf{F}_{ext} = \mathbf{M}(\ddot{q}) + \mathbf{S}(q, \dot{q}) + \mathbf{g}(q) \qquad \text{Equation } \mathbf{2}$$

which represents a system of N nonlinear equations of motion describing the dynamics for N degrees of freedom with kinematic states q. In Equation **2**, **M** includes the inertial terms, **S** the centripetal and Coriolis terms, and **g** the gravitational terms. $\mathbf{F}_{ext}$ includes the external forces and torques on the system from the suspension and hoist cables, crowding forces and torques, dig forces on the dipper, and the payload weight. Friction and other non-conservative

forces are also modelled in the representation for $\mathbf{F}_{ext}$ in Equation **2**. The equations of motion may be derived via classical mechanics using Newton-Euler, Lagrangian mechanics, or other similar considerations.

[0070] Equation **1** above expresses the tension *T* for each suspension cable **122** as a function of its fundamental resonant frequency f_0. For a plurality of *m* suspension cables each exerting a suspension force $T_m = \alpha f_0^2 + \gamma$ on the boom, it is convenient to describe the combined suspension moment *τ* on the boom as follows:

$$\tau = \boldsymbol{\upsilon}\boldsymbol{\alpha}$$

$$\tau = \begin{bmatrix} f_1^2 r_1 & f_2^2 r_2 & \dots & f_m^2 r_m & 1 \end{bmatrix} \begin{bmatrix} \alpha_1 \\ \alpha_2 \\ \vdots \\ \alpha_m \\ \delta \end{bmatrix}$$

where:

$\boldsymbol{\upsilon} \in \mathbb{R}^{1\times m+1}$ contains the frequency-squared and moment arm for each suspension cable,

$r_i = r_i(q)$;

$\boldsymbol{\alpha} \in \mathbb{R}^{m+1\times 1}$ contain length and linear density properties for each cable $\boldsymbol{\alpha_1} - \boldsymbol{\alpha_m}$ and generally corresponds to the term $\boldsymbol{\alpha}$ in Equation 1; and

δ is an aggregate bias term for the sag-extensibility and bending stiffness properties of the plurality of cables **122** and generally corresponds to the $\boldsymbol{\gamma}$ parameter in Equation 1.

[0071] The system of equations described in Equation **2** may be manipulated to derive a single nonlinear equation expressed solely as a function of the suspension moment *τ* and the corresponding shovel kinematics $q, \dot{q}$ and $\ddot{q}$ such that unknown inertial and geometric parameters $\boldsymbol{\Phi}$ are linearly separable from the nonlinear kinematic terms contained in the *n*-dimensional regressor $\mathbf{Y}(q, \dot{q}, \ddot{q})$:

$$\boldsymbol{\tau} = \boldsymbol{\upsilon}\boldsymbol{\alpha} = \mathbf{Y}\boldsymbol{\Phi} \qquad \text{Equation } \mathbf{3}$$

where:

$\mathbf{Y} \in \mathbb{R}^{1\times n}$ represents the regressor containing nonlinear functions of the shovel kinematics; and

$\boldsymbol{\Phi} \in \mathbb{R}^{n\times 1}$ contains the unknown inertial and geometric parameters of the shovel.

[0072] The parameters $\boldsymbol{\alpha}$ and $\boldsymbol{\Phi}$ in Equation **3** above are unknown but may be determined in a calibration process. Referring to Fig. **7**, a process flowchart example of a dynamic calibration process executed by the microprocessor **200** that may be implemented for the rope shovel **100** is shown generally at **700**. The process begins at block **702** when the operator controls the rope shovel **100** to cause the dipper **102** to execute a maneuvering sequence in which the crowd **116** and hoist cables **126** are extended and retracted to follow a trajectory.

[0073] Referring to Fig. **8**, the rope shovel **100** is schematically represented and the crowd **116** and hoist cables **126** are controlled to cause the dipper **102** to move along a maneuvering trajectory **800**. The calibration process involves collecting p measurement samples of the shovel's kinematics $q, \dot{q}, \ddot{q}$ and suspension cable frequencies $f_1 \ldots f_m$ while controlling the rope shovel **100** to follow the maneuvering trajectory **800** with the dipper **102** unloaded. The p samples may be represented as follows:

$$\boldsymbol{v\alpha} = \mathbf{Y\Phi} \qquad \text{Equation } \mathbf{4}$$

Which may be written as:

$$\begin{bmatrix} f_{11}^2 r_{11} & f_{21}^2 r_{21} & \cdots & f_{m1}^2 r_{m1} & 1 \\ f_{12}^2 r_{12} & f_{22}^2 r_{22} & \cdots & f_{m2}^2 r_{m2} & 1 \\ \vdots & \vdots & \ddots & \vdots & \vdots \\ f_{1p}^2 r_{1p} & f_{2p}^2 r_{2p} & \cdots & f_{mp}^2 r_{mp} & 1 \end{bmatrix} \begin{Bmatrix} \alpha_1 \\ \alpha_2 \\ \vdots \\ \alpha_4 \\ \delta \end{Bmatrix} = \begin{bmatrix} Y_{11} & Y_{21} & \cdots & Y_{n1} \\ Y_{12} & Y_{22} & \cdots & Y_{n2} \\ \vdots & \vdots & \ddots & \vdots \\ Y_{1p} & Y_{2p} & \cdots & Y_{np} \end{bmatrix} \begin{Bmatrix} \Phi_1 \\ \Phi_1 \\ \vdots \\ \Phi_n \end{Bmatrix}$$

with $\boldsymbol{v} \in \mathbb{R}^{p \times m+1}$, $\boldsymbol{\alpha} \in \mathbb{R}^{m+1 \times 1}$, $\mathbf{Y} \in \mathbb{R}^{p \times n}$, and $\boldsymbol{\Phi} \in \mathbb{R}^{n \times 1}$. To preserve the modelling assumptions, the dynamic calibration maneuver along the trajectory **800** must be performed without the dipper **102** engaging the ground or the introduction of any external forces. The maneuvering trajectory **800** is established to elicit an appropriate velocity and acceleration response in the kinematics to provide sufficient data for computations performed to solve for the unknown parameters. In one embodiment, the maneuvering trajectory **800** is established to emulate a digging operation of the rope shovel **100** and the trajectory includes lateral swing movements of the superstructure **108** (i.e. the angle q_W) with respect to the crawler track **106**.

[0074] Referring back to Fig. **7**, block **704** then directs the microprocessor **200** to receive f_o^2 values generated at block **314** of the process **300** as described above. Block **706** then directs the microprocessor **200** to receive the orientation signals generated by the attitude sensors **140 – 146** for the superstructure **108**, boom **112**, saddle **116**, and a bail hanger **130**. These values are thus generated for each of a plurality of points along the maneuvering trajectory **800** to generate a dynamic calibration dataset.

[0075] Block **708** then directs the microprocessor **200** to use the dynamic calibration dataset to solve Equation **4** for the unknown parameters via least squares:

$$\begin{aligned} \mathbf{Y}^{\dagger}\boldsymbol{v\alpha} &= \mathbf{Y}^{\dagger}\mathbf{Y\Phi} \\ \mathbf{Y}^{\dagger}\boldsymbol{v\alpha\alpha}^{+} &= \mathbf{Y}^{\dagger}\mathbf{Y\Phi\alpha}^{+} \\ \mathbf{Y}^{\dagger}\boldsymbol{v} &= \boldsymbol{\Phi\alpha}^{+} \end{aligned}$$

where $\mathbf{Y}^{\dagger}$represents the left pseudoinverse of $\mathbf{Y}$, such that $\mathbf{Y}^{\dagger}\mathbf{Y} = \mathbf{I}$, and is computed as follows:

$$\mathbf{Y}^{\dagger} = (\mathbf{Y}^{\top}\mathbf{Y})^{-1}\mathbf{Y}^{\top}$$

and $\boldsymbol{\alpha}^{+}$ represents the right pseudoinverse of $\boldsymbol{\alpha}$ such that $\boldsymbol{\alpha}\boldsymbol{\alpha}^{+} = \mathbf{I}$, and is computed as follows:

$$\boldsymbol{\alpha}^{+} = \boldsymbol{\alpha}^{\top}(\boldsymbol{\alpha}^{\top}\boldsymbol{\alpha})^{-1}$$

The unknown parameters may subsequently be lumped together as $\boldsymbol{\Pi} = \boldsymbol{\Phi}\boldsymbol{\alpha}^{+}$, where $\boldsymbol{\Pi} \in \mathbb{R}^{n\times m+1}$ and may be estimated as follows:

$$\mathbf{Y}^{\dagger}\boldsymbol{v} = \hat{\boldsymbol{\Pi}} \qquad \text{Equation 5}$$

[0076] The no-load calibration maneuver along the trajectory **800** establishes a baseline tension of the suspension cables **122** for any extension of the crowd **116** and hoist cables **126** and results in a set of no-load system parameters $\boldsymbol{\Pi}_{NL}$ being identified:

$$\boldsymbol{v}_{NL} = \mathbf{Y}\boldsymbol{\Pi}_{NL} \qquad \text{Equation 6}$$

$$\hat{\boldsymbol{\Pi}}_{NL} = \mathbf{Y}^{\dagger}\boldsymbol{v}_{NL}$$

[0077] In one embodiment the no-load system parameters may be used to determine a weight of payload in the dipper **102** based on a difference between the no-load and loaded conditions. Other digging forces such as a crowd extension force may be similarly determined.

[0078] Referring to Fig. **9**, a process flowchart example of a payload weight estimation process executed by the microprocessor **200** is shown generally at **900**. The process **900** is only executed after the kinematic parameters and dynamic parameters under no load have been determined in the calibration process **600** and **700** in Figs. 6 and 7 respectively. The process **900** begins at block **902**, which directs the microprocessor **200** to receive f_o^2 values generated at block **314** of the process **300**. Block **904** then directs the microprocessor **200** to receive the signals generated by the attitude sensors **140 – 146** for the orientation of the superstructure **108**, the boom **112**, the saddle **116**, and the bail hanger **130**. Block **906** then directs the microprocessor **200** to determine the current kinematic condition of the rope shovel **100** using the orientation signals received at block **904**. Following the kinematic calibration process **600**, the unknown kinematic parameters will have been determined and may be used to calculate the current kinematic condition of the rope shovel **100** based on the signals generated by the attitude sensors **140 – 146**.

[0079] Block **908** then directs the microprocessor **200** to determine whether the dipper **102** is in a position that facilitates estimation of a payload being carried in the dipper based on the kinematic condition of the rope shovel **100**. In one embodiment block **908** involves aspects

such as whether the payload and payload rate of change meet a threshold value and the lateral swing angular velocity and crowd **116** rectilinear and angular velocities. These determinations ensure that the dipper **102** has disengaged from the mine face **134** such that only the payload exerts an external force on the shovel components, and that the mining shovel **100** is operating within a viscous (linear) friction regime so as to neglect the contribution of nonlinear stiction effects. As an example, during active excavating of the mine face **134** the tension in the suspension cables **122** will be increased by the digging engagement forces, which would not be an appropriate time to perform payload estimation. However, immediately following the excavating operation when the dipper is not moving or moving slowly, forces acting on the dipper will be primarily due to the payload, which facilitates payload estimation. If at block **908**, the rope shovel **100** is not in a kinematic condition that facilitates payload estimation, the microprocessor **200** is directed back to block **902** and blocks **902 – 908** are repeated.

[0080] If at block **908**, the rope shovel **100** is in a kinematic condition that facilitates payload estimation, the microprocessor **200** is directed to block **910**. Block **910** directs the microprocessor **200** to calculate a payload estimation value for the current payload. For suspension moment measurements with a loaded dipper **102**, the system parameters contain payload inertial and geometric parameters encoded within $\mathbf{\Pi}_L$:

$$\boldsymbol{\upsilon}_L = \mathbf{Y}\mathbf{\Pi}_L$$

When the dipper **102** is loaded, a set of parameters may be expressed using a moment difference:

$$\begin{aligned} \boldsymbol{\upsilon}_L - \boldsymbol{\upsilon}_{NL} &= \mathbf{Y}(\mathbf{\Pi}_L - \mathbf{\Pi}_{NL}) \\ \boldsymbol{\upsilon}_L - \mathbf{Y}\mathbf{\Pi}_{NL} &= \mathbf{Y}\boldsymbol{\epsilon} \\ \Delta\boldsymbol{\upsilon} &= \mathbf{Y}\boldsymbol{\epsilon} \end{aligned}$$

Where the subscript *L* represents the loaded dipper condition and the subscript *NL* represents the unloaded dipper condition. The no-load moment may be estimated by Equation **6**, and $\boldsymbol{\epsilon} = \mathbf{\Pi}_L - \mathbf{\Pi}_{NL}$ includes only the unknown payload inertial and geometric terms. The friction parameters are assumed to be payload invariant. The term $\boldsymbol{\epsilon}$ may thus be estimated as:

$$\hat{\boldsymbol{\epsilon}} = \mathbf{Y}^{\dagger}\Delta\boldsymbol{\upsilon} \qquad \text{Equation } \mathbf{7}$$

where $\mathbf{Y}^{\dagger}$ is the left pseudoinverse of $\mathbf{Y}$. In general, $\boldsymbol{\epsilon}$ is represented by some function of the payload parameters $\boldsymbol{\rho}_p$:

$$\boldsymbol{\rho}_p = \begin{Bmatrix} m_p \\ m_p x_p \\ m_p y_p \\ I_p + m_p(x_p^2 + y_p^2) \end{Bmatrix}$$

Where m_p, x_p, y_p, and I_p correspond to the payload weight, center-of-mass positions (x_p, y_p) with respect to the dipper, and inertia for rotation in the $x_1 - z_1$ plane, respectively. The term $\boldsymbol{\epsilon}$ maybe expressed as a linear combination of $\boldsymbol{\rho}_p$ such that it is mapped via a payload Jacobian $\boldsymbol{J}_{\boldsymbol{\epsilon}}$ as a function of constant shovel geometric parameters (*BL, BV, CH*, θ_{CH}, etc.):

$$\boldsymbol{\epsilon} = \boldsymbol{J}_{\boldsymbol{\epsilon}}\boldsymbol{\rho}_p$$

Such that $\boldsymbol{\rho}_p$ may be obtained from an estimated $\hat{\epsilon}$ as follows:

$$\boldsymbol{\rho}_p = \boldsymbol{J}_{\boldsymbol{\epsilon}}{}^{\dagger}\hat{\boldsymbol{\epsilon}}$$

Where $\boldsymbol{J}_{\boldsymbol{\epsilon}}{}^{\dagger}$ represents the left pseudoinverse of $\boldsymbol{J}_{\boldsymbol{\epsilon}}$. Combining this with Equation **7** above, $\boldsymbol{\rho}_p$ and therefore the payload weight may be calculated as follows:

$$\widehat{\boldsymbol{\rho}}_p = \boldsymbol{J}_{\epsilon}^{\dagger}\mathbf{Y}_l^{\dagger}\Delta\boldsymbol{v}$$

[0081] The determined payload weight may be displayed on the display **250** in the operator's cab **110** on an ongoing basis to provide the operator with a real-time assessment of a loaded payload weight. The payload weight over time may also be recorded for further analysis to determine operator performance and/or digging effectiveness in bucket fill per load and loading truck fill.

[0082] Language of degree used herein, such as the terms "approximately," "about," "generally," and "substantially" as used herein represent a value, amount, or characteristic close to the stated value, amount, or characteristic that still performs a desired function or achieves a desired result. For example, the terms "approximately", "about", "generally," and "substantially" may refer to an amount that is within less than 10 % of, within less than 5 % of, within less than 1 % of, within less than 0.1 % of, or within less than 0.01 % of the stated value.

[0083] While specific embodiments have been described and illustrated, such embodiments should be considered illustrative only and not as limiting the disclosed embodiments.

CLAIMS:

1. A method for monitoring a mining shovel having a boom supported by a plurality of suspension cables, the method comprising:

receiving accelerometer signals from a plurality of accelerometers, each accelerometer being mounted on one of the plurality of suspension cables;

processing the accelerometer signals to extract a fundamental frequency associated with vibrations in each suspension cable, the fundamental frequency being proportional to a tension in the suspension cable; and

determining changes in the fundamental frequency as a function of time, the changes facilitating a determination of an operating state of the mining shovel.

2. The method of claim **1** wherein receiving the accelerometer signals comprises receiving accelerometer signals from an accelerometer mounted on the suspension cable at a distance of at least one-third of the length from an end of the suspension cable.

3. The method of any one of claims **1-2** wherein determining changes in the fundamental frequency comprises detecting changes in fundamental frequency that are indicative of a boom jacking event associated with an excavation being performed by the rope shovel.

4. The method of any one of claims **1-3** wherein determining changes in the fundamental frequency comprises determining changes in fundamental frequency that are indicative of a potential failure of one of the plurality of suspension cables.

5. The method of claim **4** further comprising determining a tension in each of the plurality of suspension cables based on the respective fundamental frequencies relating the fundamental frequency to tension.

6. The method of any one of claims **1-5** further comprising estimating forces on components of the mining shovel by:

receiving orientation signals from one or more attitude sensors associated with the components, the orientation signals defining an orientation of the components;

determining a kinematic condition defining the position and orientation of the components based on the orientation signals and kinematic calibration data; and

determining forces acting on the components of the mining shovel based on the kinematic condition, the orientation signals, and the fundamental frequency tension in each of the plurality of suspension cables.

7. The method of claim **6** wherein estimating the forces on components of the mining shovel comprises estimating a weight of a payload in a payload container component of the mining shovel.

8. The method of claim **6** further comprising performing a kinematic calibration to establish the kinematic calibration data by:

controlling the mining shovel to cause one of the components of the shovel to be successively located in each of a plurality of known positions and orientations with respect to the mining shovel; and

processing the orientation signals based on the plurality of known positions and orientations to determine the kinematic calibration data for the mining shovel.

9. The method of claim **6**, wherein determining forces acting on the components of the mining shovel further includes performing a dynamic calibration to establish dynamic calibration data by:

causing an unloaded payload container component of the mining shovel to maneuver through a trajectory while receiving the orientation signals and determining the changes in the fundamental frequency; and

determining forces on the components of the mining shovel under unloaded conditions based on the changes in fundamental frequency.

10. The method of claim **9** wherein the trajectory is selected to emulate a digging operation of the mining shovel.

11. A monitoring system for monitoring a mining shovel having a boom supported by a plurality of suspension cables, the system comprising:

an accelerometer being mounted on one of the plurality of suspension cables at a distance of at least one-third of the length from an end of the suspension cable; and

a processor in communication with the accelerometer includes programmable logic to process the accelerometer signals to extract a fundamental frequency associated with vibrations in the suspension cable, the fundamental frequency being proportional to a tension in the suspension cable; and determine changes in the fundamental frequency as a function of time, the changes facilitating a determination of an operating state of the mining shovel.

12. The monitoring system of claim **11**, wherein the processor includes programmable logic to detect changes in fundamental frequency that are indicative of a boom jacking event associated with an excavation being performed by the rope shovel.

13. The monitoring system of claim **11** or **12**, wherein the processor includes programmable logic to detect changes in fundamental frequency that are indicative of a potential failure of one of the plurality of suspension cables.

14. The monitoring system of any one of claims **11-13**, further comprising

one or more attitude sensors associated with the boom and other components of the mining shovel, the one or more attitude sensors sending orientation signals defining an orientation of the components;

the processor having programmable logic to determine a kinematic condition defining the position and orientation of the components based on the orientation signals; and

the processor having programmable logic to determine forces acting on the components of the mining shovel based on the kinematic condition, the orientation signals, and the fundamental frequency tension in each of the plurality of suspension cables.

15. The monitoring system of any one of claims **11-14**, wherein estimating the forces on components of the mining shovel comprises estimating a weight of a payload in a payload container component of the mining shovel.

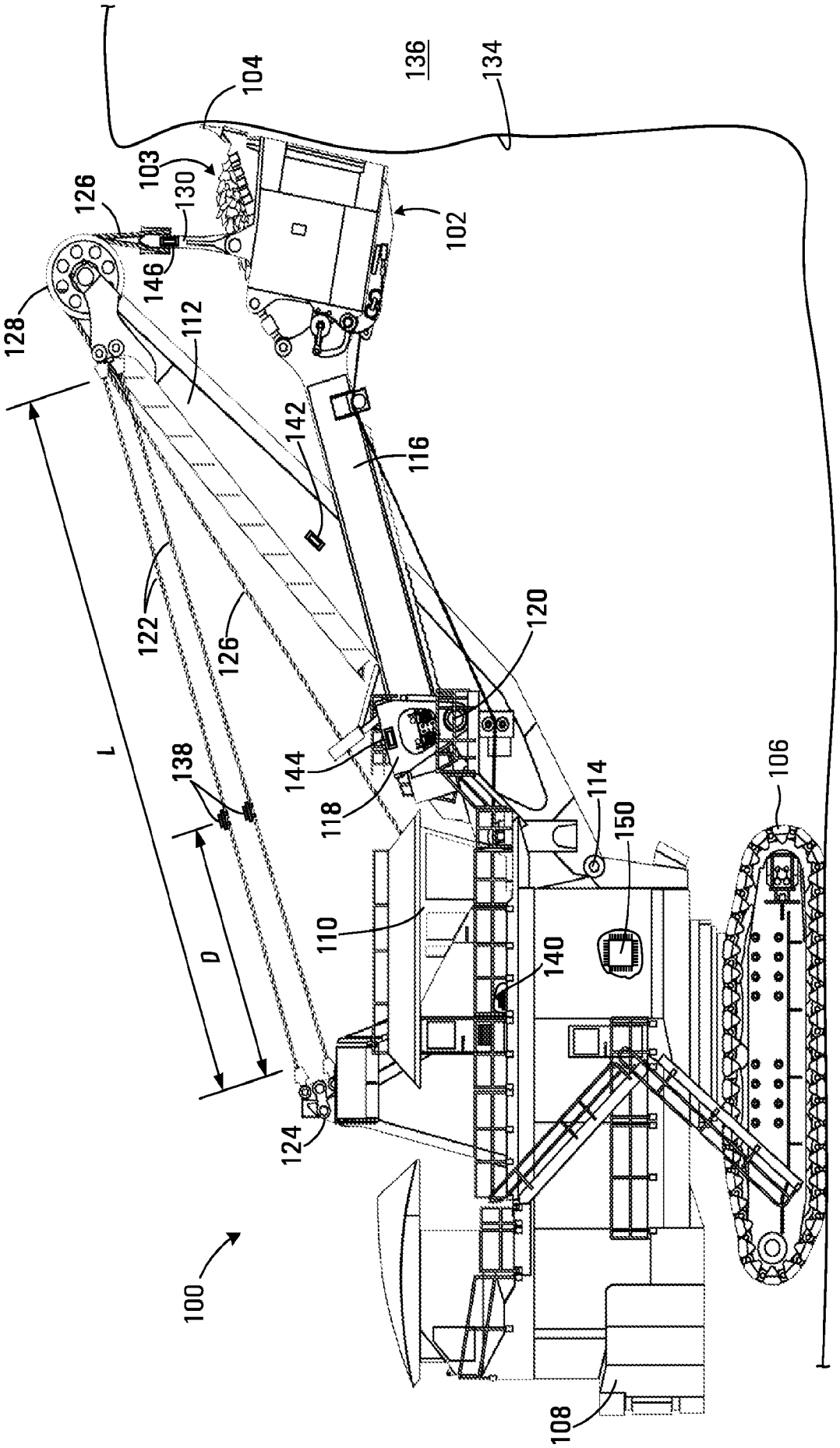
104
136
134
103
130
126
102
146
128
112
142
116
122
126
120
L
138
144
118
114
106
150
D
110
140
124
100
108

FIG. 1A

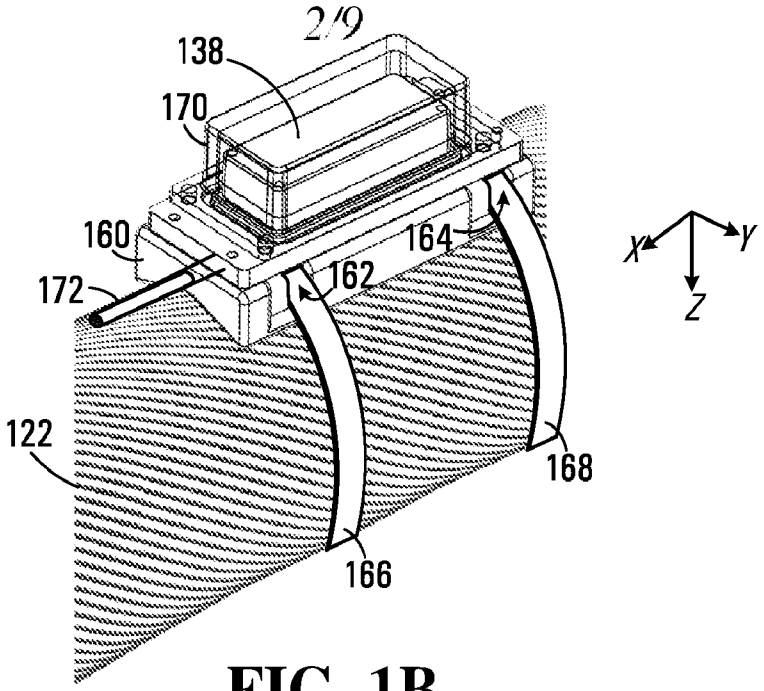
2/9
138
170
160
172
164
162
122
168
166
X
Y
Z

FIG. 1B

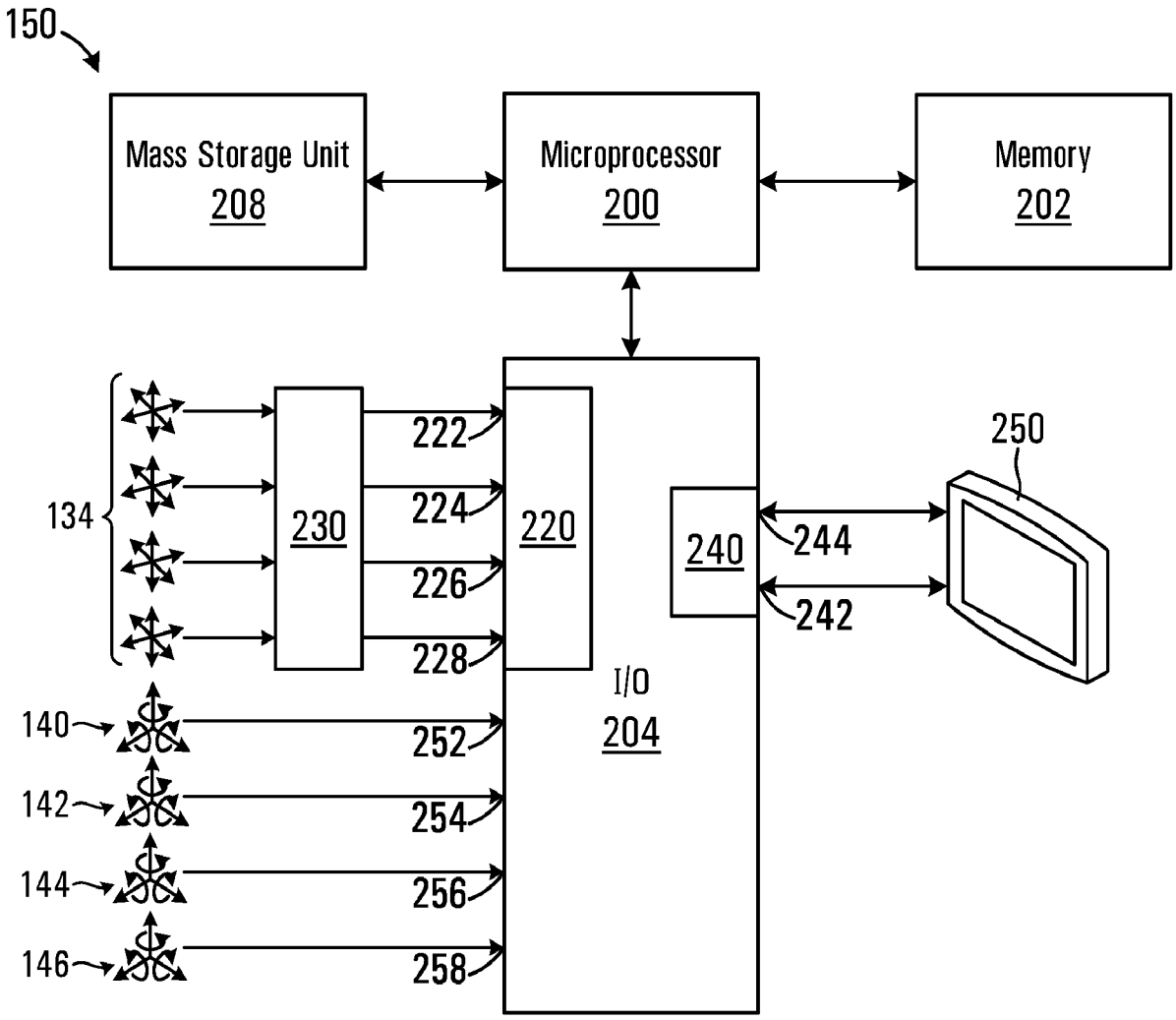
150
Mass Storage Unit
208
Microprocessor
200
Memory
202
134
230
222
224
226
228
220
240
244
242
250
I/O
204
140
142
144
146
252
254
256
258

FIG. 2

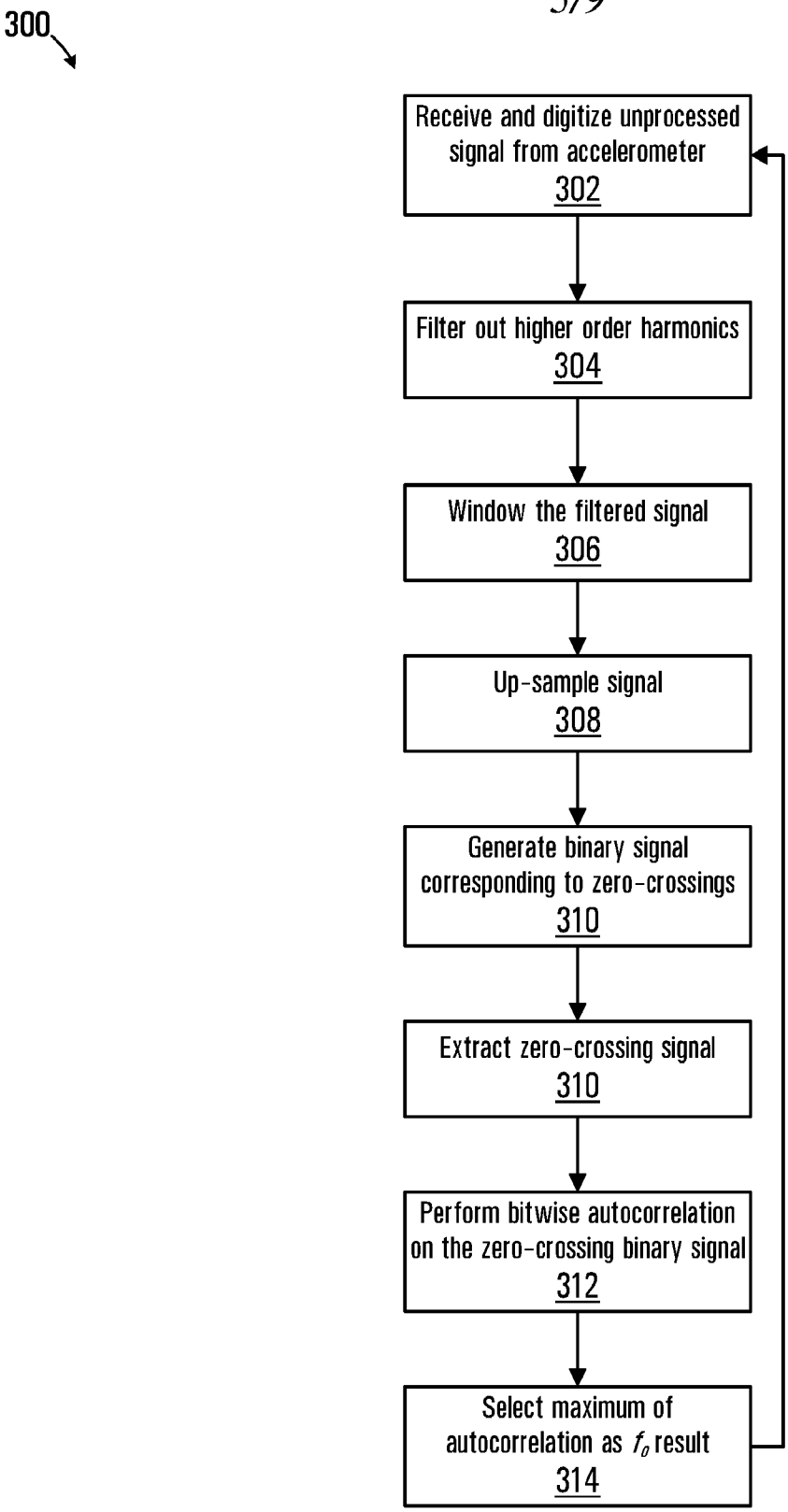
300
Receive and digitize unprocessed signal from accelerometer
302
Filter out higher order harmonics
304
Window the filtered signal
306
Up-sample signal
308
Generate binary signal corresponding to zero-crossings
310
Extract zero-crossing signal
310
Perform bitwise autocorrelation on the zero-crossing binary signal
312
Select maximum of autocorrelation as f_0 result
314

FIG. 3

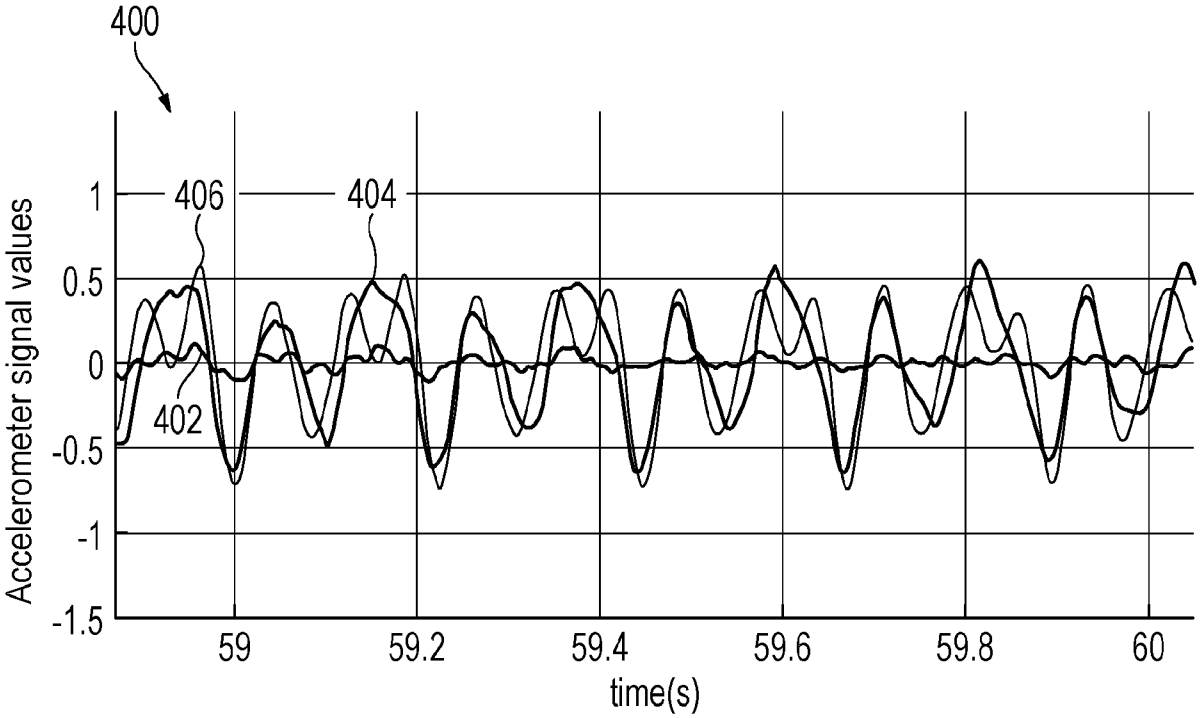
400
406
404
402
Accelerometer signal values
1
0.5
0
-0.5
-1
-1.5
59
59.2
59.4
59.6
59.8
60
time(s)

FIG. 4A

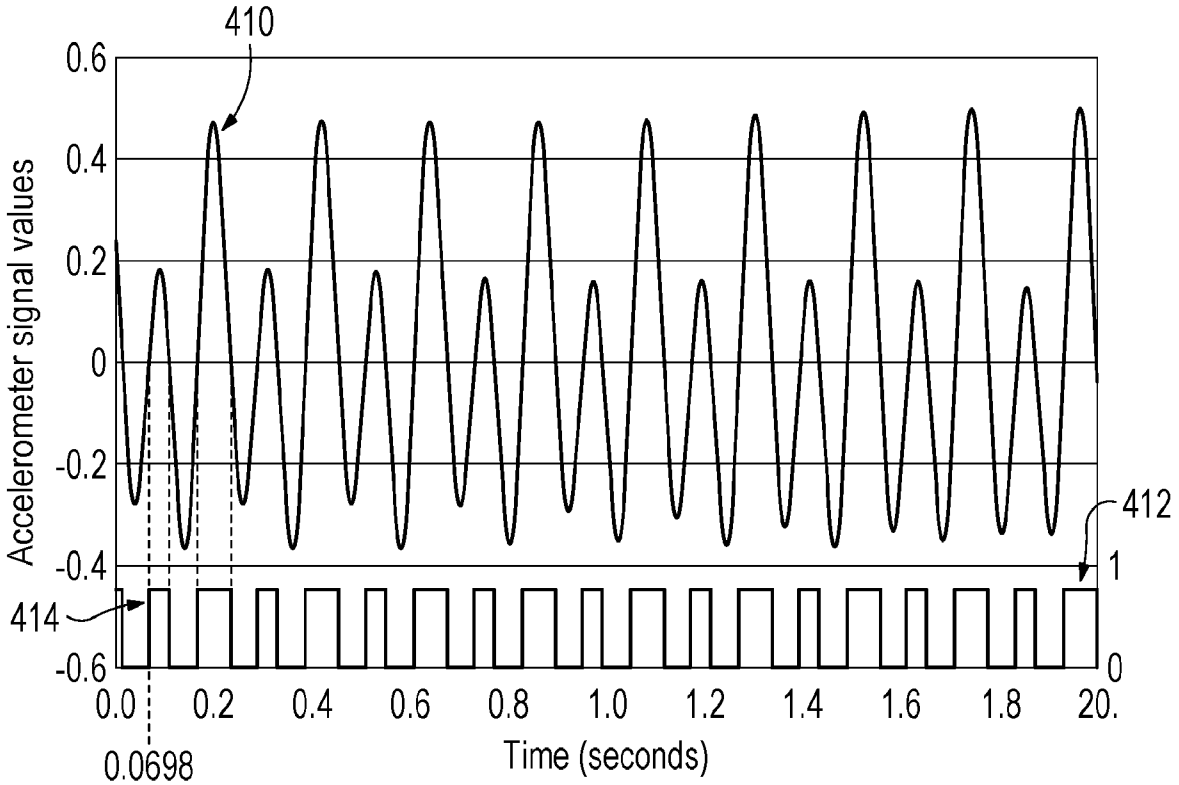
410
0.6
0.4
0.2
0
-0.2
-0.4
-0.6
Accelerometer signal values
412
1
0
414
0.0
0.2
0.4
0.6
0.8
1.0
1.2
1.4
1.6
1.8
20.
0.0698
Time (seconds)

FIG. 4B

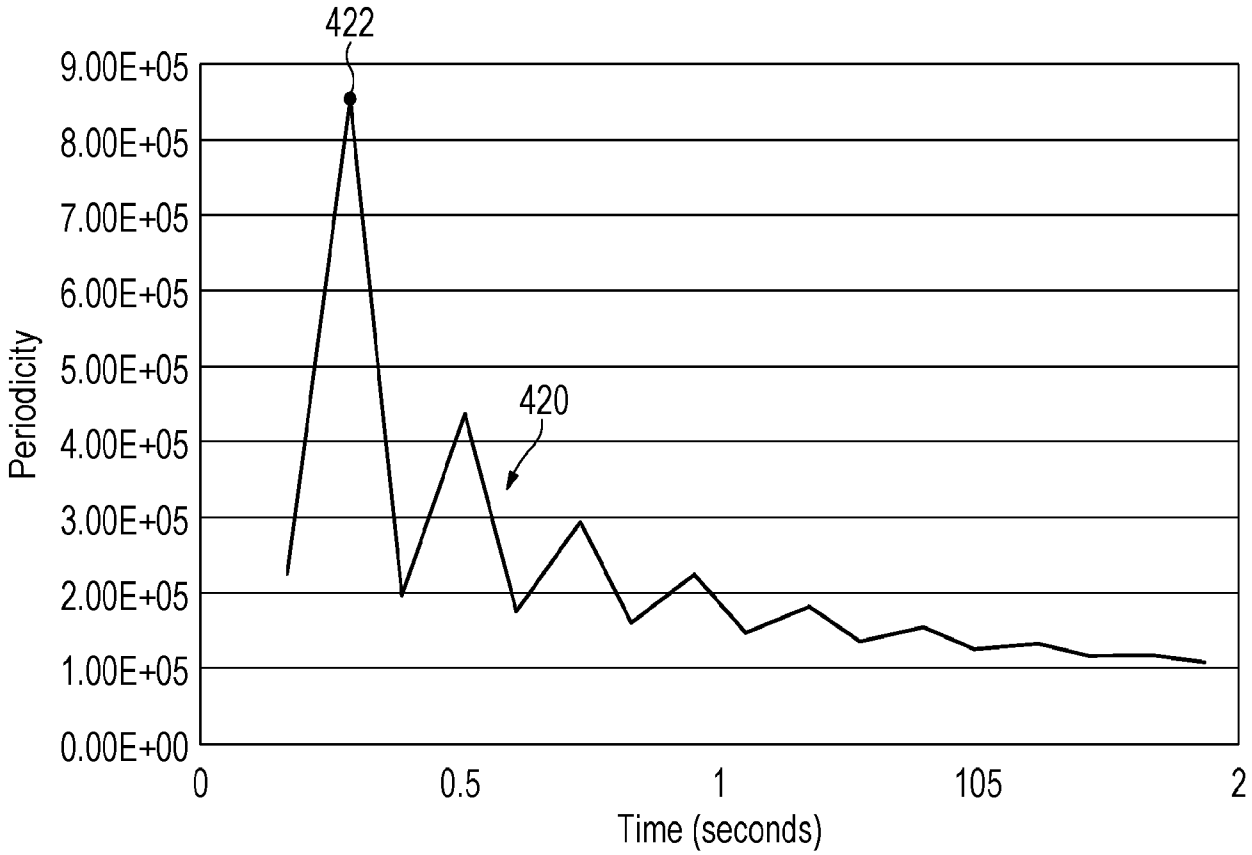
422
420
9.00E+05
8.00E+05
7.00E+05
6.00E+05
5.00E+05
4.00E+05
3.00E+05
2.00E+05
1.00E+05
0.00E+00
Periodicity
0
0.5
1
105
2
Time (seconds)

FIG. 4C

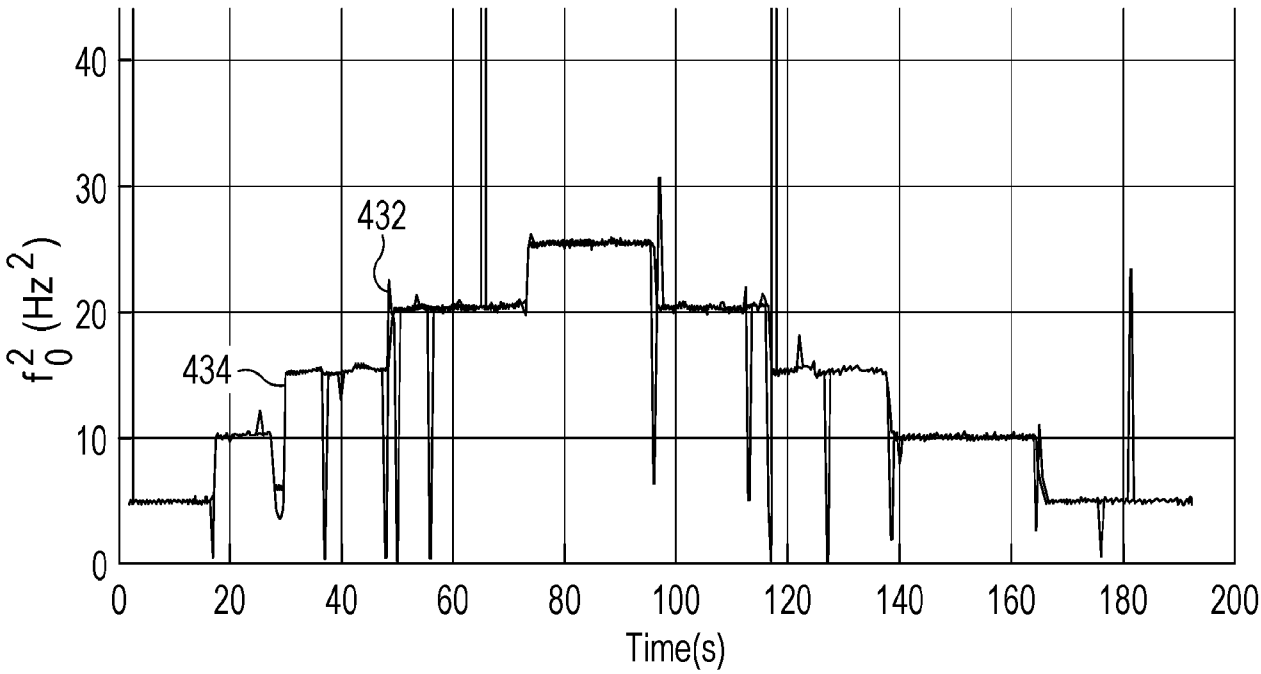
40
30
20
10
0
f_0^2 (Hz^2)
432
434
0
20
40
60
80
100
120
140
160
180
200
Time(s)

FIG. 4D

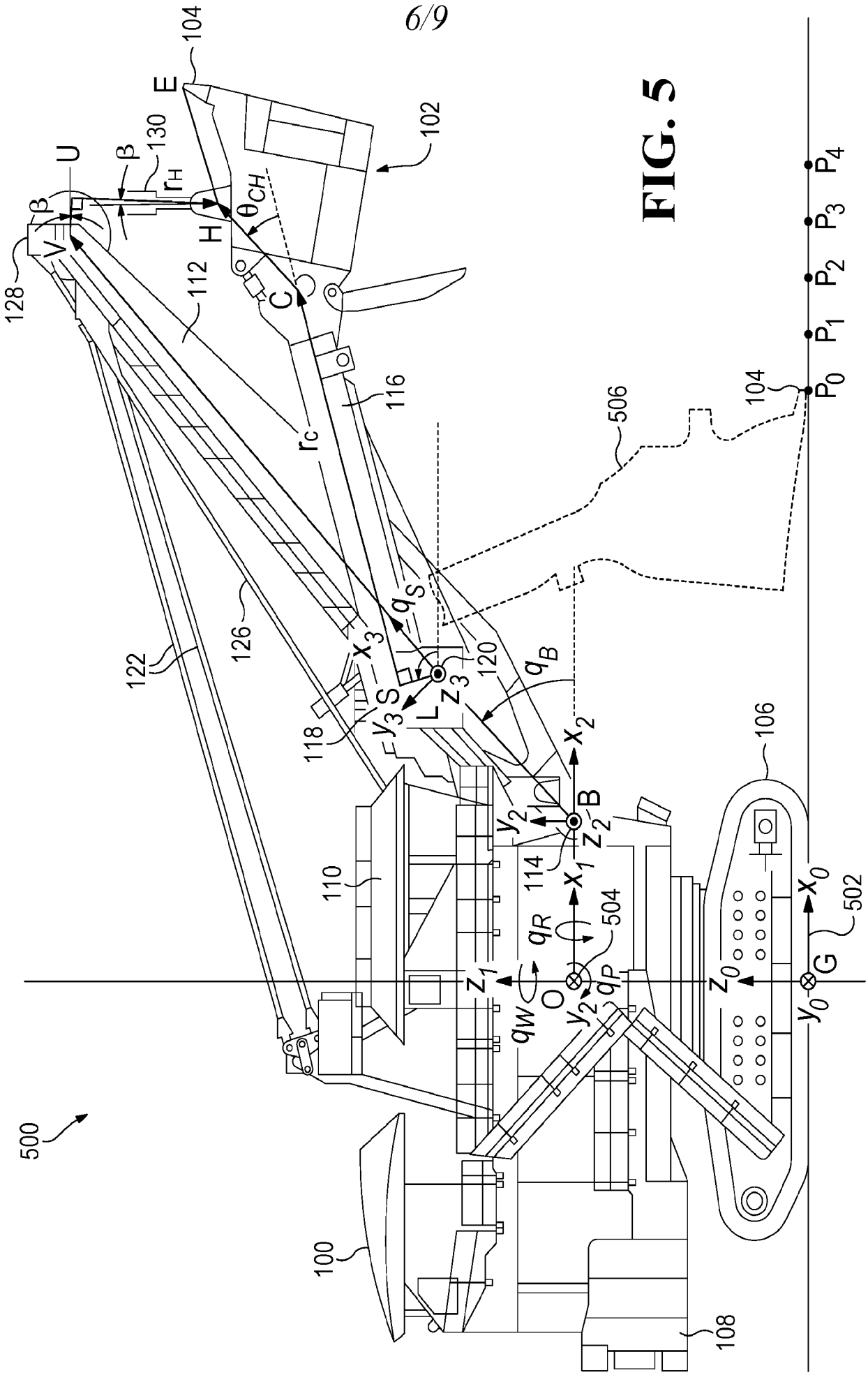
500
100
102
104
106
108
110
112
114
116
118
120
122
126
128
130
502
504
506
E
U
V
H
C
L
S
B
G
O
β
r_H
r_c
θ_{CH}
q_S
q_B
q_R
q_P
q_W
x_3
y_3
z_3
x_2
y_2
z_2
x_1
y_1
z_1
x_0
y_0
z_0
P_0
P_1
P_2
P_3
P_4

FIG. 5

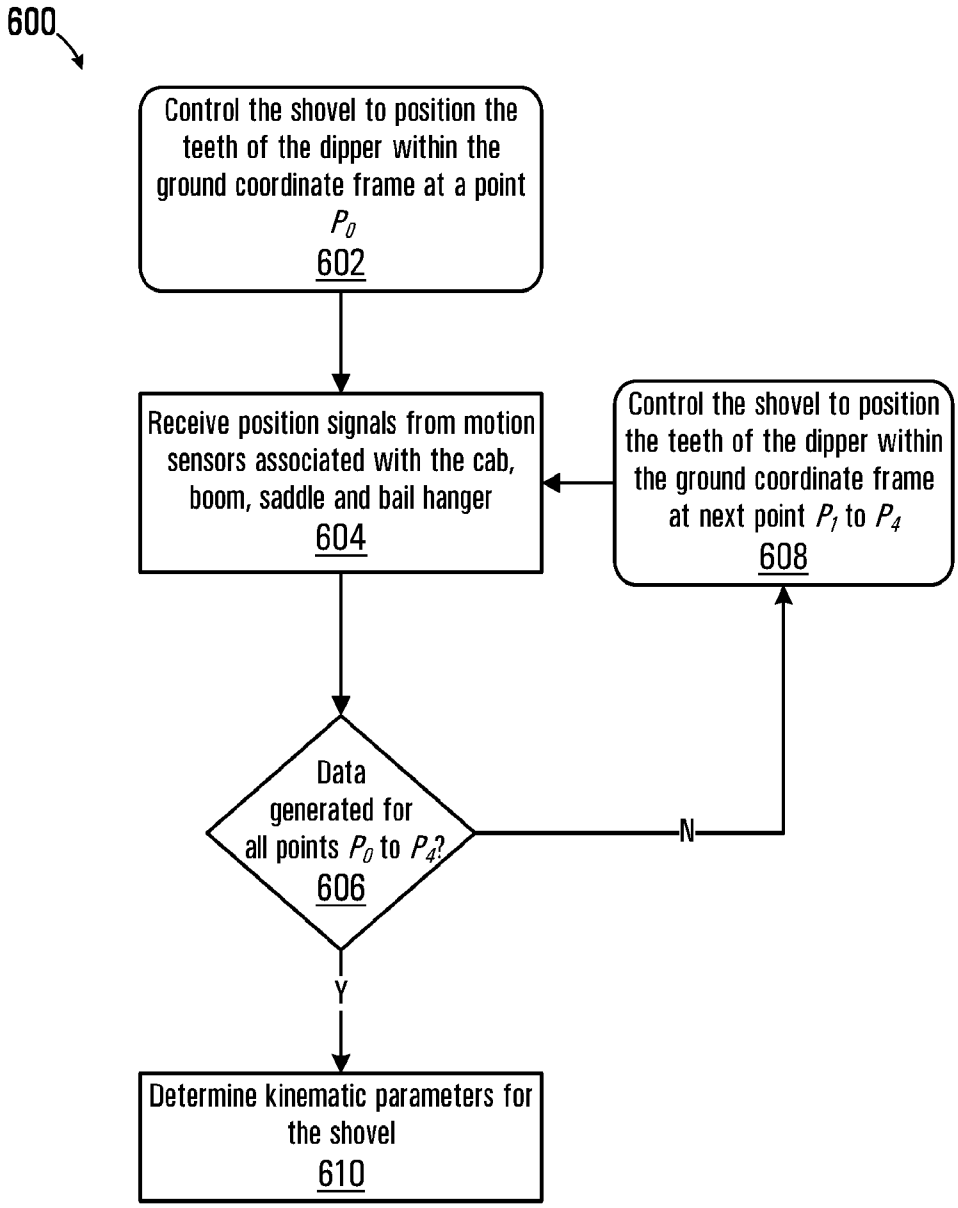
600
Control the shovel to position the teeth of the dipper within the ground coordinate frame at a point P_0
602
Receive position signals from motion sensors associated with the cab, boom, saddle and bail hanger
604
Control the shovel to position the teeth of the dipper within the ground coordinate frame at next point P_1 to P_4
608
Data generated for all points P_0 to P_4?
606
N
Y
Determine kinematic parameters for the shovel
610

FIG. 6

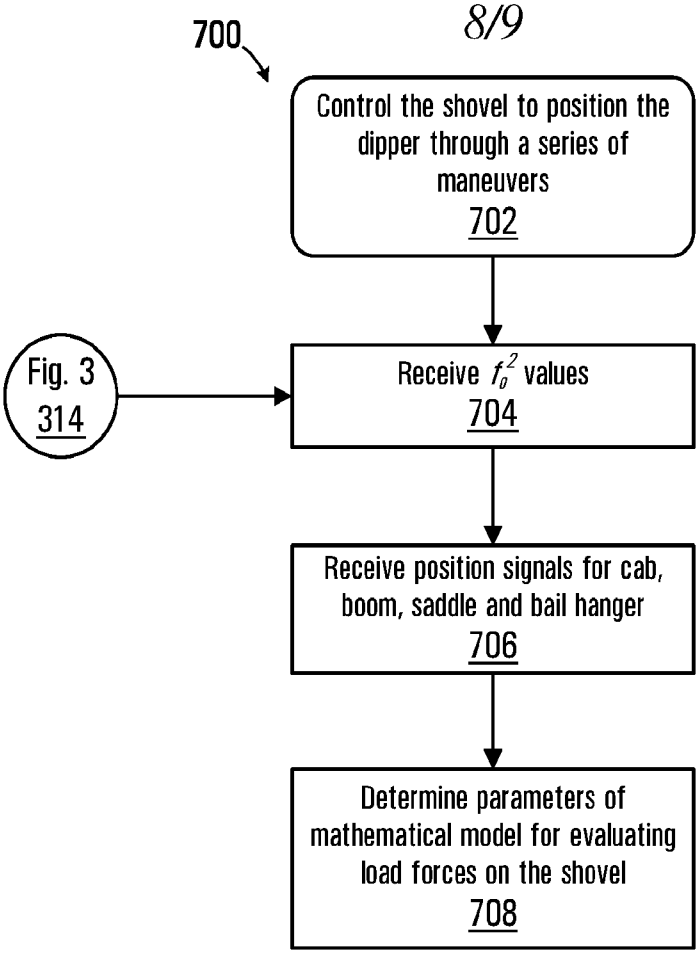
700
Control the shovel to position the dipper through a series of maneuvers
702
Fig. 3
314
Receive f_0^2 values
704
Receive position signals for cab, boom, saddle and bail hanger
706
Determine parameters of mathematical model for evaluating load forces on the shovel
708

FIG. 7

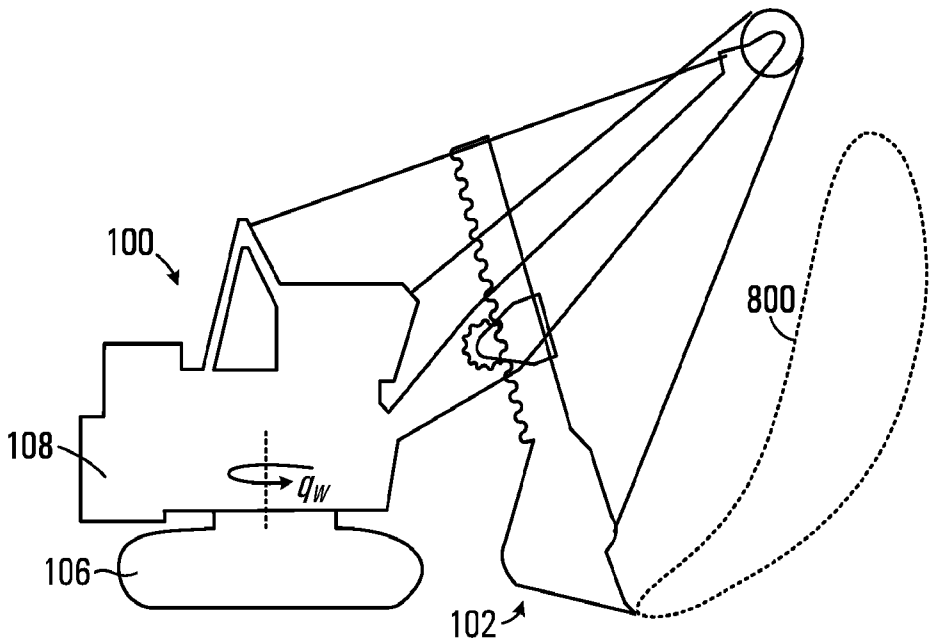
100
800
108
q_W
106
102

FIG. 8

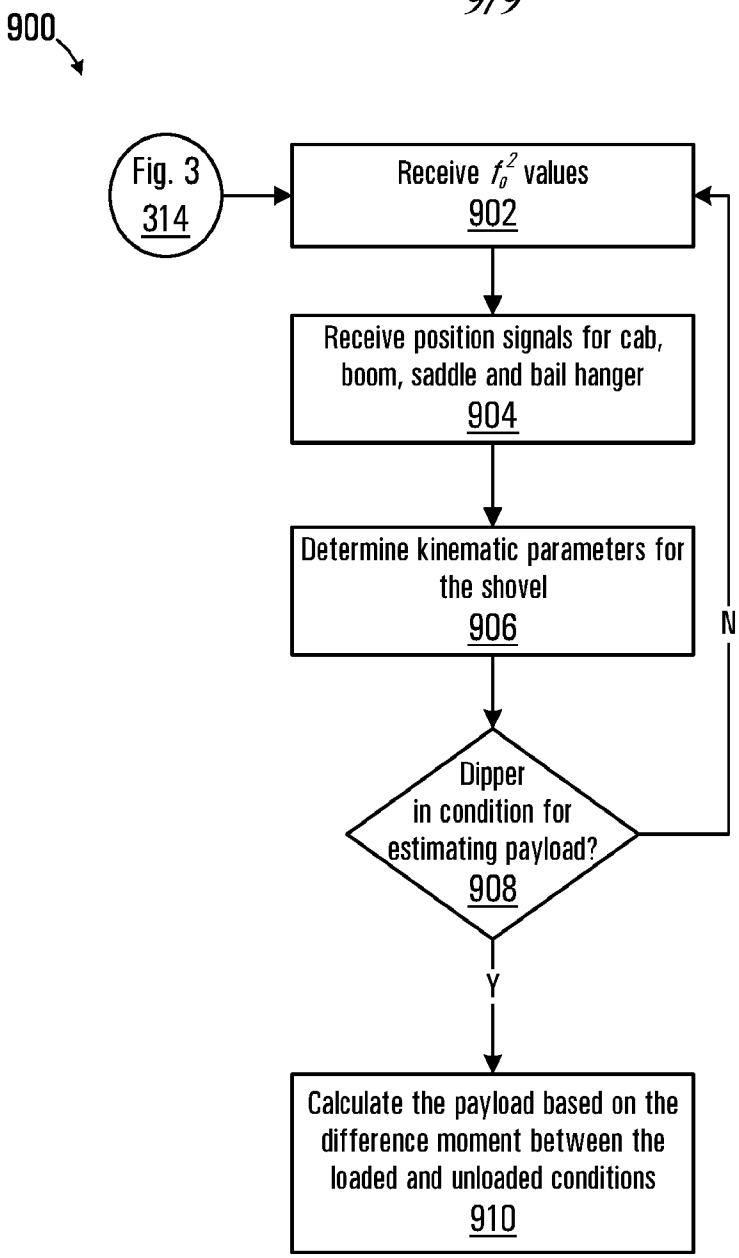
900
Fig. 3
314
Receive f_0^2 values
902
Receive position signals for cab, boom, saddle and bail hanger
904
Determine kinematic parameters for the shovel
906
Dipper in condition for estimating payload?
908
N
Y
Calculate the payload based on the difference moment between the loaded and unloaded conditions
910

FIG. 9

INTERNATIONAL SEARCH REPORT

International application No.
PCT/US2023/031437

A. CLASSIFICATION OF SUBJECT MATTER

E02F 9/14(2006.01)i
FI: E02F9/14 Z

According to International Patent Classification (IPC) or to both national classification and IPC

B. FIELDS SEARCHED

Minimum documentation searched (classification system followed by classification symbols)

E02F9/14

Documentation searched other than minimum documentation to the extent that such documents are included in the fields searched

Published examined utility model applications of Japan 1922-1996
Published unexamined utility model applications of Japan 1971-2023
Registered utility model specifications of Japan 1996-2023
Published registered utility model applications of Japan 1994-2023

Electronic data base consulted during the international search (name of data base and, where practicable, search terms used)

C. DOCUMENTS CONSIDERED TO BE RELEVANT

Category*	Citation of document, with indication, where appropriate, of the relevant passages	Relevant to claim No.
A	US 2018/0066414 A1 (HARNISCHFEGER TECHNOLOGIES, INC) 08 March 2018 (2018-03-08)	1-15
A	JP 2018-001282 A (YASKAWA INFORMATION SYSTEMS CORPORATION) 11 January 2018 (2018-01-11)	1-15
A	Microfilm of the specification and drawings annexed to the written application of Japanese Utility Model Application No.57269/1990(Laid-open No.17445/1992) (TAMURA Manabu) 13.02.1992 (1992-02-13)	1-15

☐ Further documents are listed in the continuation of Box C. ☑ See patent family annex.

* Special categories of cited documents:
"A" document defining the general state of the art which is not considered to be of particular relevance
"E" earlier application or patent but published on or after the international filing date
"L" document which may throw doubts on priority claim(s) or which is cited to establish the publication date of another citation or other special reason (as specified)
"O" document referring to an oral disclosure, use, exhibition or other means
"P" document published prior to the international filing date but later than the priority date claimed
"T" later document published after the international filing date or priority date and not in conflict with the application but cited to understand the principle or theory underlying the invention
"X" document of particular relevance; the claimed invention cannot be considered novel or cannot be considered to involve an inventive step when the document is taken alone
"Y" document of particular relevance; the claimed invention cannot be considered to involve an inventive step when the document is combined with one or more other such documents, such combination being obvious to a person skilled in the art
"&" document member of the same patent family

Date of the actual completion of the international search	Date of mailing of the international search report
29 November 2023	**12 December 2023**
Name and mailing address of the ISA/JP **Japan Patent Office** **3-4-3, Kasumigaseki, Chiyoda-ku, Tokyo** **100-8915, Japan**	Authorized officer **YUMOTO, Teruki 2B 9404** Telephone No. **+81-3-3581-1101 Ext. 3237**

INTERNATIONAL SEARCH REPORT
Information on patent family members

International application No.
PCT/US2023/031437

Patent document cited in search report	Publication date (day/month/year)	Patent family member(s)	Publication date (day/month/year)
US 2018/0066414 A1	08 March 2018	CA 2978389 A1	
		CN 107806123 A	
JP 2018-001282 A	11 January 2018	(Family: none)	
JP 17445/1992 U1	13 February 1992	(Family: none)	